

PITHA 94/37

hep-ph/9409396

September, 1994

# Energy Spectra and Energy Correlations in the Decay $H \rightarrow ZZ \rightarrow \mu^+\mu^-\mu^+\mu^-$

Torsten Arens and L. M. Sehgal

III. Physikalisches Institut (A), RWTH Aachen,  
D-52074 Aachen, Germany

## Abstract

It is shown that in the sequential decay  $H \rightarrow ZZ \rightarrow (f_1\bar{f}_1) + (f_2\bar{f}_2)$ , the energy distribution of the final state particles provides a simple and powerful test of the  $HZZ$  vertex. For a standard Higgs boson, the energy spectrum of any final fermion, in the rest frame of  $H$ , is predicted to be  $d\Gamma/dx \sim 1 + \beta^4 - 2(x - 1)^2$ , with  $\beta = \sqrt{1 - 4m_Z^2/m_H^2}$  and  $1 - \beta \leq x = 4E/m_H \leq 1 + \beta$ . By contrast, the spectrum for a pseudoscalar Higgs is  $d\Gamma/dx \sim \beta^2 + (x - 1)^2$ . There are characteristic energy correlations between  $f_1$  and  $f_2$  and between  $f_1$  and  $\bar{f}_2$ . These considerations are applied to the “gold-plated” reaction  $H \rightarrow ZZ \rightarrow \mu^+\mu^-\mu^+\mu^-$ , including possible effects of  $CP$ -violation in the  $HZZ$  coupling. Our formalism also yields the energy spectra and correlations of leptons in the decay  $H \rightarrow W^+W^- \rightarrow l^+\nu_l l^-\bar{\nu}_l$ .

# 1 Introduction

One of the distinctive signatures of a Higgs particle with mass  $m_H > 2m_Z$  is the sequential decay

$$H \rightarrow ZZ \rightarrow (\mu^+\mu^-) + (\mu^+\mu^-). \quad (1)$$

The observation of such a four-muon final state, consisting of two  $\mu^+\mu^-$  pairs with the invariant mass of the  $Z$ , together resonating at some invariant mass  $m_H$ , would be unmistakable evidence for a particle with the *prima facie* characteristics of the Higgs boson [1].

In the standard model, the Higgs boson has the quantum numbers  $J^{PC} = 0^{++}$ , and a very specific form of coupling to gauge bosons, namely  $g_{\mu\nu}\varepsilon_1^\mu\varepsilon_2^\nu$ . (We denote the polarization vectors and momenta of the two  $Z$  bosons by  $(\varepsilon_1, p_1)$  and  $(\varepsilon_2, p_2)$ .) More generally, a scalar  $0^{++}$  particle can couple to a pair of  $Z$ 's according to  $(Bg_{\mu\nu} + \frac{C}{m_Z^2}p_{1\nu}p_{2\mu})\varepsilon_1^\mu\varepsilon_2^\nu$ . In extended gauge models, there are also pseudoscalar Higgs particles with quantum numbers  $0^{-+}$ ; these can have radiatively induced couplings to two  $Z$  bosons of the form  $\frac{D}{m_Z^2}\varepsilon_{\mu\nu\rho\sigma}\varepsilon_1^\mu\varepsilon_2^\nu p_1^\rho p_2^\sigma$  [2, 3, 4].

The purpose of this paper is to show that in decays of the type

$$H \rightarrow ZZ \rightarrow (f_1\bar{f}_1) + (f_2\bar{f}_2), \quad (2)$$

of which Eq. (1) is an example, the energy spectrum of the final fermions, in the rest frame of the  $H$ , is a simple and powerful probe of the  $HZZ$  vertex. This is highlighted by the following result (to be obtained in Section 3): For a standard Higgs boson, the energy spectrum of any final fermion (independent of whether it is a lepton,  $u$ -quark or  $d$ -quark) has the universal form

$$\frac{1}{\Gamma} \frac{d\Gamma}{dx} = \frac{3/(2\beta)}{3 - 2\beta^2 + 3\beta^4} [1 + \beta^4 - 2(x - 1)^2] \quad (\text{Scalar Higgs}), \quad (3)$$

where  $x = 4E/m_H$ ,  $\beta = \sqrt{1 - 4m_Z^2/m_H^2}$  and the range of  $x$  is  $1 - \beta \leq x \leq 1 + \beta$ .

By contrast, for a pseudoscalar Higgs boson, the spectrum is

$$\frac{1}{\Gamma} \frac{d\Gamma}{dx} = \frac{3}{8\beta^3} [\beta^2 + (x-1)^2] \quad (\text{Pseudoscalar Higgs}). \quad (4)$$

This difference between  $0^{++}$  and  $0^{-+}$  Higgs decays is exhibited in Fig. 1, for  $m_H = 300$  GeV.

We will derive in this paper the energy spectrum of the reaction (2) for a general  $HZZ$  coupling. In addition to single particle spectra, we will obtain the correlated two-particle energy distribution of  $f_1$  and  $f_2$ , and of  $f_1$  and  $\bar{f}_2$ . In Section 3, we consider Higgs couplings of the scalar and pseudoscalar form, as well as  $CP$ -violating effects when both are present simultaneously. In Section 4, we will relate the energy characteristics of the reactions (1) and (2) to the helicity wave-function of the  $ZZ$  system created in the decay  $H \rightarrow ZZ$ .

Our work is complementary to other analyses devoted to the sequential decays  $H \rightarrow ZZ \rightarrow (f_1\bar{f}_1) + (f_2\bar{f}_2)$ , in which the structure of the  $HZZ$  coupling is probed by means of the angular distribution of the final particles, particularly the correlation between the  $f_1\bar{f}_1$  and  $f_2\bar{f}_2$  planes [2] - [9]. Our formalism allows us also to obtain the energy spectrum and correlation of leptons produced in the decay  $H \rightarrow W^+W^- \rightarrow l^+\nu_l l^-\bar{\nu}_l$ , which we have reported earlier [10].

## 2 Differential Decay Rate

Consider the sequential decay

$$H(P) \rightarrow Z(p_1)Z(p_2) \rightarrow f_1(q_1)\bar{f}_1(q_2)f_2(q_3)\bar{f}_2(q_4) \quad (5)$$

induced by a general  $HZZ$  coupling

$$A[H \rightarrow Z(\varepsilon_1, p_1) + Z(\varepsilon_2, p_2)] = 2im_Z^2 \sqrt{G_F \sqrt{2}} \left[ Bg_{\mu\nu} + \frac{C}{m_Z^2} p_{1\nu} p_{2\mu} \right]$$

$$+ \frac{D}{m_Z^2} \varepsilon_{\mu\nu\rho\sigma} p_1^\rho p_2^\sigma \Big] \varepsilon_1^{*\mu} \varepsilon_2^{*\nu}. \quad (6)$$

The differential decay rate is given by

$$\begin{aligned} d^8\Gamma = & \frac{8\sqrt{2}G_F^3 m_Z^4 D_Z}{m_H} (v_1^2 + a_1^2)(v_2^2 + a_2^2) \left[ |B|^2 \mathcal{S} + \frac{|C|^2}{m_Z^4} \mathcal{L} + \frac{\text{Re}(B^*C)}{m_Z^2} \mathcal{M} \right. \\ & + \frac{\text{Im}(B^*C)}{m_Z^2} \mathcal{N} + \frac{|D|^2}{m_Z^4} \mathcal{P} + \frac{\text{Re}(B^*D)}{m_Z^2} \mathcal{Q} + \frac{\text{Im}(B^*D)}{m_Z^2} \mathcal{R} \\ & \left. + \frac{\text{Re}(C^*D)}{m_Z^4} \mathcal{U} + \frac{\text{Im}(C^*D)}{m_Z^4} \mathcal{V} \right] \cdot dLips, \end{aligned} \quad (7)$$

where, neglecting fermion masses,

$$\begin{aligned} \mathcal{S} &= (q_1 \cdot q_3)(q_2 \cdot q_4) + (q_1 \cdot q_4)(q_2 \cdot q_3) + \xi_1 \xi_2 \left( (q_1 \cdot q_3)(q_2 \cdot q_4) - (q_1 \cdot q_4)(q_2 \cdot q_3) \right), \\ \mathcal{L} &= 2 \left( (p_2 \cdot q_1)(p_2 \cdot q_2) - \frac{m_Z^4}{4} \right) \left( (p_1 \cdot q_3)(p_1 \cdot q_4) - \frac{m_Z^4}{4} \right), \\ \mathcal{M} &= (p_2 \cdot q_1) \left( (p_1 \cdot q_3)(q_2 \cdot q_4) + (p_1 \cdot q_4)(q_2 \cdot q_3) \right) \\ &+ (p_2 \cdot q_2) \left( (p_1 \cdot q_3)(q_1 \cdot q_4) + (p_1 \cdot q_4)(q_1 \cdot q_3) \right) - \frac{m_Z^4}{4} (p_1 \cdot p_2) \\ &+ \xi_1 \xi_2 \left[ (p_1 \cdot p_2) \left( (q_1 \cdot q_3)(q_2 \cdot q_4) - (q_1 \cdot q_4)(q_2 \cdot q_3) \right) \right. \\ &\quad \left. - \frac{m_Z^4}{4} \left( (q_1 - q_2) \cdot (q_3 - q_4) \right) \right], \\ \mathcal{N} &= \varepsilon(q_1, q_2, q_3, q_4) \left[ \xi_1 \left( p_1 \cdot (q_4 - q_3) \right) + \xi_2 \left( p_2 \cdot (q_2 - q_1) \right) \right], \\ \mathcal{P} &= -\frac{m_Z^8}{8} - 2 \left( (q_1 \cdot q_3)(q_2 \cdot q_4) - (q_1 \cdot q_4)(q_2 \cdot q_3) \right)^2 \\ &+ \frac{m_Z^4}{4} \left[ \left( (q_1 \cdot q_3) + (q_2 \cdot q_4) \right)^2 + \left( (q_1 \cdot q_4) + (q_2 \cdot q_3) \right)^2 \right] \\ &+ \xi_1 \xi_2 \frac{m_Z^4}{4} \left[ \left( (q_1 \cdot q_3) - (q_2 \cdot q_4) \right)^2 - \left( (q_1 \cdot q_4) - (q_2 \cdot q_3) \right)^2 \right], \\ \mathcal{Q} &= \varepsilon(q_1, q_2, q_3, q_4) \left[ \left( (q_1 - q_2) \cdot (q_4 - q_3) \right) - \xi_1 \xi_2 (p_1 \cdot p_2) \right], \\ \mathcal{R} &= (\xi_1 + \xi_2) \left[ \left( (q_1 \cdot q_3) - (q_2 \cdot q_4) \right) \left( \frac{m_Z^4}{4} + (q_1 \cdot q_3)(q_2 \cdot q_4) - (q_1 \cdot q_4)(q_2 \cdot q_3) \right) \right] \\ &+ (\xi_1 - \xi_2) \left[ \left( (q_1 \cdot q_4) - (q_2 \cdot q_3) \right) \left( \frac{m_Z^4}{4} + (q_1 \cdot q_4)(q_2 \cdot q_3) - (q_1 \cdot q_3)(q_2 \cdot q_4) \right) \right], \\ \mathcal{U} &= \varepsilon(q_1, q_2, q_3, q_4) \left[ \left( p_1 \cdot (q_3 - q_4) \right) \left( p_2 \cdot (q_2 - q_1) \right) - \xi_1 \xi_2 \left( (p_1 \cdot p_2)^2 - m_Z^4 \right) \right], \end{aligned}$$

$$\begin{aligned}\mathcal{V} = & \left[ \xi_1(p_1 \cdot (q_3 - q_4)) + \xi_2(p_2 \cdot (q_1 - q_2)) \right] \left[ \frac{m_Z^4}{4} \left( (q_1 - q_2) \cdot (q_4 - q_3) \right) \right. \\ & \left. + (p_1 \cdot p_2) \left( (q_1 \cdot q_3)(q_2 \cdot q_4) - (q_1 \cdot q_4)(q_2 \cdot q_3) \right) \right],\end{aligned}\quad (8)$$

and  $dLips$  is the Lorentz invariant phase space element

$$dLips = (2\pi)^4 \delta^{(4)}(P - q_1 - q_2 - q_3 - q_4) \prod_{i=1}^4 \frac{d^3 q_i}{(2\pi)^3 2q_i^0}. \quad (9)$$

The factor  $D_Z$  in Eq. (7) is the product of the two  $Z$  boson propagators,

$$D_Z = m_Z^4 \prod_{j=1}^2 \frac{1}{(p_j^2 - m_Z^2)^2 + m_Z^2 \Gamma_Z^2}, \quad (10)$$

which, in the narrow-width approximation, may be written as

$$D_Z \approx \frac{\pi^2 m_Z^2}{\Gamma_Z^2} \delta(p_1^2 - m_Z^2) \delta(p_2^2 - m_Z^2). \quad (11)$$

The parameters  $\xi_1$  and  $\xi_2$  are given by

$$\xi_i = \frac{2v_i a_i}{v_i^2 + a_i^2}, \quad i = 1, 2 \quad (12)$$

where  $v_i$  and  $a_i$  are the vector and axial vector coupling constants of the fermion pair  $f_i \bar{f}_i$  to  $Z$  ( $v_f = 2I_f^3 - 4e_f \sin^2 \Theta_W$ ,  $a_f = 2I_f^3$ ). Eq. (7) is the basis of all the results to be obtained in the following Sections.

### 3 Energy Spectra and Correlations: Scalar vs. Pseudoscalar Higgs and $CP$ -Violation

We consider an  $HZZ$  coupling that is a combination of  $B$ - and  $D$ -type terms in Eq. (6), with  $C = 0$ . This will enable us to compare a scalar Higgs ( $B \neq 0$ ,  $D = 0$ ) with a pseudoscalar Higgs ( $B = 0$ ,  $D \neq 0$ ), as well as discuss certain  $CP$ -violating effects arising from simultaneous presence of both terms.

For the reaction  $H \rightarrow ZZ \rightarrow (f_1\bar{f}_1) + (f_2\bar{f}_2)$ , with  $f_1 \neq f_2$ , we obtain the following energy distributions for the pairs  $(f_1, f_2)$ ,  $(\bar{f}_1, \bar{f}_2)$ ,  $(\bar{f}_1, f_2)$  and  $(f_1, \bar{f}_2)$ :

$$\begin{aligned}
\frac{1}{\Gamma} \frac{d\Gamma}{dx(\overset{(-)}{f_1}) dx'(\overset{(-)}{f_2})} &= \frac{1}{N} \left\{ |B|^2 (F_1 + \xi_1 \xi_2 F_2) + |D|^2 (F_3 + \xi_1 \xi_2 F_4) \right. \\
&\quad \left. + \text{Im}(B^* D) [\xi_1 (F_5 + F_6) + \xi_2 (F_5 - F_6)] \right\}, \\
\frac{1}{\Gamma} \frac{d\Gamma}{dx(\bar{f}_1) dx'(f_2)} &= \frac{1}{N} \left\{ |B|^2 (F_1 - \xi_1 \xi_2 F_2) + |D|^2 (F_3 - \xi_1 \xi_2 F_4) \right. \\
&\quad \left. - \text{Im}(B^* D) [\xi_1 (F_5 + F_6) - \xi_2 (F_5 - F_6)] \right\}, \\
\frac{1}{\Gamma} \frac{d\Gamma}{dx(f_1) dx'(\bar{f}_2)} &= \frac{1}{N} \left\{ |B|^2 (F_1 - \xi_1 \xi_2 F_2) + |D|^2 (F_3 - \xi_1 \xi_2 F_4) \right. \\
&\quad \left. + \text{Im}(B^* D) [\xi_1 (F_5 + F_6) - \xi_2 (F_5 - F_6)] \right\}, \tag{13}
\end{aligned}$$

with the normalization factor

$$N = |B|^2 (3 - 2\beta^2 + 3\beta^4) + 8|D|^2 \beta^2. \tag{14}$$

The functions  $F_i$  are defined as follows

$$\begin{aligned}
F_1(x, x') &= \frac{9}{32\beta^6} \left\{ (1 - \beta^2)^2 [\beta^2 + (x - 1)^2] [\beta^2 + (x' - 1)^2] \right. \\
&\quad \left. + 2(1 + \beta^2)^2 [\beta^2 - (x - 1)^2] [\beta^2 - (x' - 1)^2] \right\}, \\
F_2(x, x') &= \frac{9}{8\beta^4} (1 - \beta^2)^2 (x - 1)(x' - 1), \\
F_3(x, x') &= \frac{9}{8\beta^4} [\beta^2 + (x - 1)^2] [\beta^2 + (x' - 1)^2], \\
F_4(x, x') &= 4\beta^2 F_2(x, x') / (1 - \beta^2)^2, \\
F_5(x, x') &= \frac{9(1 - \beta^2)}{8\beta^4} (x + x' - 2) [(x - 1)(x' - 1) + \beta^2], \\
F_6(x, x') &= \frac{9(1 - \beta^2)}{8\beta^4} (x' - x) [(x - 1)(x' - 1) - \beta^2]. \tag{15}
\end{aligned}$$

Note that  $F_{1,\dots,5}$  are symmetric under exchange of  $x$  and  $x'$ , while  $F_6$  is antisymmetric.

By integrating the two-particle distributions (13) over the energies of one of the particles, we obtain the inclusive energy spectrum of any fermion  $f$  in the decay  $H \rightarrow ZZ \rightarrow f\bar{f} + \dots$ :

$$\frac{1}{\Gamma} \frac{d\Gamma}{dx(\overset{(-)}{f})} = \frac{3}{2\beta N} \left\{ |B|^2 [1 + \beta^4 - 2(x-1)^2] + 2|D|^2 [\beta^2 + (x-1)^2] \right. \\ \left. + \overset{(+)}{4\text{Im}(B^*D)\xi(1-\beta^2)(x-1)} \right\}. \quad (16)$$

For a pure scalar ( $B$ -type) or pseudoscalar ( $D$ -type) Higgs coupling, we obtain the results already announced in Eqs. (3) and (4).

Although the two-particle distributions given in Eq. (13) were derived for the reaction  $H \rightarrow ZZ \rightarrow (f_1\bar{f}_1) + (f_2\bar{f}_2)$  with  $f_1 \neq f_2$ , the results are also applicable to the decay  $H \rightarrow ZZ \rightarrow (\mu^+\mu^-) + (\mu^+\mu^-)$ . The only requirement is that the two observed muons belong to different  $Z$ 's. This is automatically the case for like sign pairs  $\mu^+\mu^+$  or  $\mu^-\mu^-$ , and is easy to ensure for  $\mu^+\mu^-$  by requiring that their invariant mass be different from  $m_Z$ . (Note that a  $\mu^+\mu^-$  pair from the same  $Z$  must fulfil  $x + x' = 2$ .) With this proviso the correlated energy distributions for  $\mu^+\mu^+$ ,  $\mu^-\mu^-$  and  $\mu^+\mu^-$  are

$$\frac{1}{\Gamma} \frac{d\Gamma}{dx(\mu^\pm)dx'(\mu^\pm)} = \frac{1}{N} [ |B|^2 (F_1 + \xi^2 F_2) + |D|^2 (F_3 + \xi^2 F_4) \mp 2\text{Im}(B^*D)\xi F_5 ], \\ \frac{1}{\Gamma} \frac{d\Gamma}{dx(\mu^\pm)dx'(\mu^\mp)} = \frac{1}{N} [ |B|^2 (F_1 - \xi^2 F_2) + |D|^2 (F_3 - \xi^2 F_4) \mp 2\text{Im}(B^*D)\xi F_6 ]. \quad (17)$$

Here  $\xi = 2va/(v^2 + a^2) \approx 0.16$  is the parameter describing the  $Z$  coupling to muons.

From Eqs. (17), we draw the following conclusions.

(i) For a scalar Higgs coupling ( $D = 0$ ), the like sign muon pairs  $\mu^+\mu^+$  and  $\mu^-\mu^-$  have the energy distribution

$$\frac{1}{\Gamma} \frac{d\Gamma}{dx(\mu^\pm)dx'(\mu^\pm)} = \frac{1}{3 - 2\beta^2 + 3\beta^4} [F_1(x, x') + \xi^2 F_2(x, x')] \quad (\text{Scalar Higgs}). \quad (18)$$

This is quite distinct from the pseudoscalar Higgs decay, given by

$$\frac{1}{\Gamma} \frac{d\Gamma}{dx(\mu^\pm)dx'(\mu^\pm)} = \frac{1}{8\beta^2} [F_3(x, x') + \xi^2 F_4(x, x')] \quad (\text{Pseudoscalar Higgs}). \quad (19)$$

These two distributions are contrasted in Fig. 2.

- (ii) The unlike sign dimuon  $\mu^+ \mu^-$  spectra are likewise quite different for  $0^{++}$  and  $0^{-+}$  Higgs decays. Indeed, the  $\mu^+ \mu^-$  spectra differ from the  $\mu^\pm \mu^\pm$  given in Eqs. (18) and (19) only in the replacement  $\xi^2 \rightarrow -\xi^2$ . Since  $\xi^2$  is approximately  $2.56 \times 10^{-2}$ , the two-dimensional distributions for unlike sign  $\mu$ 's are very similar to those of the like sign muon pairs, shown in Fig. 2.
- (iii) The simultaneous presence of  $B$ - and  $D$ -type couplings produces a  $CP$ -violating asymmetry between  $\mu^+ \mu^+$  and  $\mu^- \mu^-$ . There is also an asymmetry between the single particle  $\mu^+$  and  $\mu^-$  spectra, that can be read off Eq. (16):

$$\begin{aligned} A &= \frac{d\Gamma/dx(\mu^-) - d\Gamma/dx(\mu^+)}{d\Gamma/dx(\mu^-) + d\Gamma/dx(\mu^+)} \\ &= \text{Im}(B^*D) \frac{4\xi(x-1)(1-\beta^2)}{|B|^2[1+\beta^4-2(x-1)^2] + 2|D|^2[\beta^2+(x-1)^2]}. \end{aligned} \quad (20)$$

It should be noted that all of these asymmetries are odd under  $CP$  but even under  $T$ . Thus they require a non-zero phase difference between the amplitudes  $B$  and  $D$ , induced by final state interactions. This is evident from the appearance of the factor  $\text{Im}(B^*D)$  in the asymmetric terms in Eq. (17), and in Eq. (20). The asymmetries are also proportional to the parameter  $\xi$ , which is approximately 0.16 for muon pairs.

## 4 Energy Spectra and Correlations: Relation to Helicity Structure of $H \rightarrow ZZ$ Amplitude

Quite generally, the decay  $H \rightarrow ZZ$  produces a system of two  $Z$  bosons in the helicity state

$$|ZZ\rangle = c_+|++\rangle + c_-|--\rangle + c_0|00\rangle. \quad (21)$$

Couplings of the form  $B$ ,  $C$  and  $D$  (Eq. (6)) give rise to the following characteristic helicity wave-functions:

$$\begin{aligned} B g_{\mu\nu} \varepsilon_1^\mu \varepsilon_2^\nu &: |++\rangle + |--\rangle + \frac{1+\beta^2}{1-\beta^2} |00\rangle \\ \frac{C}{m_Z^2} p_{1\nu} p_{2\mu} \varepsilon_1^\mu \varepsilon_2^\nu &: |00\rangle \\ \frac{D}{m_Z^2} \varepsilon_{\mu\nu\rho\sigma} p_1^\rho p_2^\sigma \varepsilon_1^\mu \varepsilon_2^\nu &: |++\rangle - |--\rangle. \end{aligned} \quad (22)$$

Notice that the standard Higgs boson coupling generates a transversely polarized state  $|++\rangle + |--\rangle$  mixed with a specific amount of longitudinal polarization  $|00\rangle$ . In the high energy limit  $\beta \rightarrow 1$ , the longitudinal component dominates. In comparison, a pseudoscalar Higgs decays into a transversely polarized state  $|++\rangle - |--\rangle$ . A scalar coupling of the form  $\frac{C}{m_Z^2} p_{1\nu} p_{2\mu} \varepsilon_1^\mu \varepsilon_2^\nu$  generates a state of longitudinal polarization  $|00\rangle$  only.

It is possible to relate the energy distributions derived in the preceding Section to the helicity structure of the  $H \rightarrow ZZ$  amplitude. To this end, it is important to note (i) that, as far as the energy distributions are concerned, the transverse and longitudinal components of the  $ZZ$  wave-function add incoherently; (ii) that the energy spectra do not distinguish between the states  $|++\rangle + |--\rangle$  and  $|++\rangle - |--\rangle$ . In the  $CP$ -invariant limit, therefore, the energy distribution of the final fermion system can be written as follows:

(a) One-dimensional distribution

$$\frac{1}{\Gamma} \frac{d\Gamma}{dx} = P_T f_T(x) + P_L f_L(x), \quad (23)$$

where  $P_T$  and  $P_L$  are the probabilities for transverse and longitudinal polarization in the  $ZZ$  wave-function ( $P_T + P_L = 1$ ), and  $x$  is the scaled energy ( $x = 4E/m_H$ ) of *any* of the final fermions in  $H \rightarrow ZZ \rightarrow (f_1 \bar{f}_1) + (f_2 \bar{f}_2)$ . The functions  $f_T$  and  $f_L$  are given by

$$\begin{aligned} f_T(x) &= \frac{3}{8\beta^3} [\beta^2 + (x-1)^2], \\ f_L(x) &= \frac{3}{4\beta^3} [\beta^2 - (x-1)^2]. \end{aligned} \quad (24)$$

(b) Two-dimensional distribution

$$\frac{1}{\Gamma} \frac{d\Gamma}{dxdx'} = P_T [f_T(x)f_T(x') \pm \xi_1 \xi_2 g_T(x)g_T(x')] + P_L [f_L(x)f_L(x')], \quad (25)$$

with

$$g_T(x) = \frac{3}{4\beta^2} (x-1). \quad (26)$$

In Eq. (25), the  $+$  sign applies to a pair  $(f_1, f_2)$  or  $(\bar{f}_1, \bar{f}_2)$ , while the  $-$  sign applies to a pair  $(f_1, \bar{f}_2)$ . It is easy to see that Eqs. (23) to (26) reproduce the results (13) and (16), in the limit of  $CP$ -conservation.

It is clear from the structure of Eq. (25) that, for  $P_T \neq 0$ , the two-dimensional distribution is not simply a product of one-dimensional spectra. The term proportional to  $g_T(x)g_T(x')$  is indicative of the fact that the transverse helicities of the two  $Z$ 's are *correlated*. On the other hand, for  $P_T = 0$ , the two-particle distribution factorises into a product of one-particle spectra. The three types of coupling in Eq.

(22) are obviously characterised by:

$$\begin{aligned}
B - \text{type} &: P_T = \frac{2(1 - \beta^2)^2}{3 - 2\beta^2 + 3\beta^4} \quad , \quad P_L = \frac{(1 + \beta^2)^2}{3 - 2\beta^2 + 3\beta^4} \\
C - \text{type} &: \quad \quad P_T = 0 \quad \quad \quad , \quad \quad \quad P_L = 1 \\
D - \text{type} &: \quad \quad P_T = 1 \quad \quad \quad , \quad \quad \quad P_L = 0.
\end{aligned} \tag{27}$$

## 5 Remarks on the Decay $H \rightarrow W^+W^- \rightarrow \mu^+\nu_\mu\mu^-\bar{\nu}_\mu$

Our results for the sequential decay  $H \rightarrow ZZ \rightarrow \mu^+\mu^-\mu^+\mu^-$  are immediately adaptable to the reaction

$$H \rightarrow W^+W^- \rightarrow \mu^+\nu_\mu\mu^-\bar{\nu}_\mu. \tag{28}$$

One has only to put  $\xi_{1,2} = 1$  in Eqs. (13) or (16), and interpret  $\beta$  as  $\sqrt{1 - 4m_W^2/m_H^2}$ . If the  $W^+W^-$  state is characterised by probabilities  $P_T$  and  $P_L$  for transverse and longitudinal polarization, the one-particle spectrum of  $\mu^+$  or  $\mu^-$  (in the  $CP$ -conserving limit) is *identical* to that produced by  $H \rightarrow ZZ$ , namely the spectrum given by Eq. (23). On the other hand the correlated  $\mu^+\mu^-$  distribution in reaction (28) differs significantly from that in  $H \rightarrow ZZ \rightarrow \mu^+\mu^-\mu^+\mu^-$ , since it is obtained from Eq. (25) with  $\xi_1\xi_2 = 1$  instead of  $\xi_1\xi_2 \approx 2.56 \times 10^{-2}$ . This gives rise to a marked difference between the two reactions as illustrated in Fig. 3, for the case of a standard Higgs boson, and in Fig. 4 for the case of a pseudoscalar Higgs. Our results concerning the energy distribution of the secondary leptons in  $H \rightarrow W^+W^- \rightarrow l^+\nu_l l^-\bar{\nu}_l$  coincide with those that we have reported in an earlier paper [10].

Acknowledgements: We acknowledge useful discussions with Udo Gieseler, and collaboration on a related paper. One of us (T.A.) is recipient of a stipend from the state of Nordrhein Westfalen. The support of the German Ministry of Research and Technology (BMFT) is acknowledged with gratitude.

## References

- [1] J.F. Gunion, H.E. Haber, G. Kane and S. Dawson, *The Higgs Hunter's Guide* (Addison–Wesley Publishing Company, 1990)
- [2] C.A. Nelson, Phys. Rev. D37 (1988) 1220
- [3] A. Soni and R.M. Xu, Phys. Rev. D48 (1993) 5259
- [4] D. Chang and W.-Y. Keung, Phys. Lett. B305 (1993) 261
- [5] D. Chang, W.-Y. Keung and I. Phillips, Phys. Rev. D48 (1993) 3225
- [6] A. Skjold and P. Osland, Phys. Lett. B311 (1993) 261; Phys. Lett. B329 (1994) 305
- [7] V. Barger, K. Cheung, A. Djouadi, B.A. Kniehl and P.M. Zerwas, Phys. Rev. D49 (1994) 79; M. Krämer, J. Kühn, M.L. Stong and P.M. Zerwas, DESY preprint 93-174
- [8] T. Matsuura and J.J. van der Bij, Z. Phys. C51 (1991) 259
- [9] A. Djouadi and B.A. Kniehl, in  *$e^+e^-$  Collisions at 500 GeV: The Physics Potential*, Proceedings of the Workshop – Munich, Annecy, Hamburg, edited by P.M. Zerwas (DESY report 93-123C)
- [10] T. Arens, U.D.J. Gieseler and L.M. Sehgal, “Energy correlation and asymmetry of secondary leptons originating in  $H \rightarrow t\bar{t}$  and  $H \rightarrow W^+W^-$ ”, Aachen preprint PITPA 94/25, to appear in Phys. Lett. B

## Figure Captions

Fig. 1. Single particle energy spectra of a fermion  $f$  in the decay  $H \rightarrow ZZ \rightarrow f + \dots$

The full curve represents the scalar case and the dashed curve the pseudoscalar case, for  $m_H = 300$  GeV.

Fig. 2. Normalized energy distribution of like sign muon pairs  $\mu^+\mu^+$  or  $\mu^-\mu^-$  in the decay  $H \rightarrow ZZ \rightarrow \mu^+\mu^-\mu^+\mu^-$ . Fig. 2(a) shows the spectrum of a standard model Higgs boson, and Fig. 2(b) that of a pseudoscalar Higgs, with  $m_H = 300$  GeV.

Fig. 3. Normalized energy distribution of unlike sign muon pairs  $\mu^+\mu^-$  in the decay of a standard model Higgs boson with mass  $m_H = 200$  GeV. (a)  $\mu^+\mu^-$  distribution in  $H \rightarrow ZZ \rightarrow \mu^+\mu^-\mu^+\mu^-$ , with  $\mu^+$  and  $\mu^-$  chosen from different  $Z$ 's; (b)  $\mu^+\mu^-$  distribution in  $H \rightarrow W^+W^- \rightarrow \mu^+\nu_\mu\mu^-\bar{\nu}_\mu$ .

Fig. 4. Normalized energy distribution of unlike sign  $\mu^+\mu^-$  pairs in the decay of a pseudoscalar Higgs boson ( $m_H = 200$  GeV). (a)  $\mu^+\mu^-$  distribution in  $H \rightarrow ZZ \rightarrow \mu^+\mu^-\mu^+\mu^-$ , with  $\mu^+$  and  $\mu^-$  chosen from different  $Z$ 's; (b)  $\mu^+\mu^-$  distribution in  $H \rightarrow W^+W^- \rightarrow \mu^+\nu_\mu\mu^-\bar{\nu}_\mu$ .

$$\Gamma^{-1} d\Gamma/dx (H \rightarrow ZZ \rightarrow f + \dots)$$

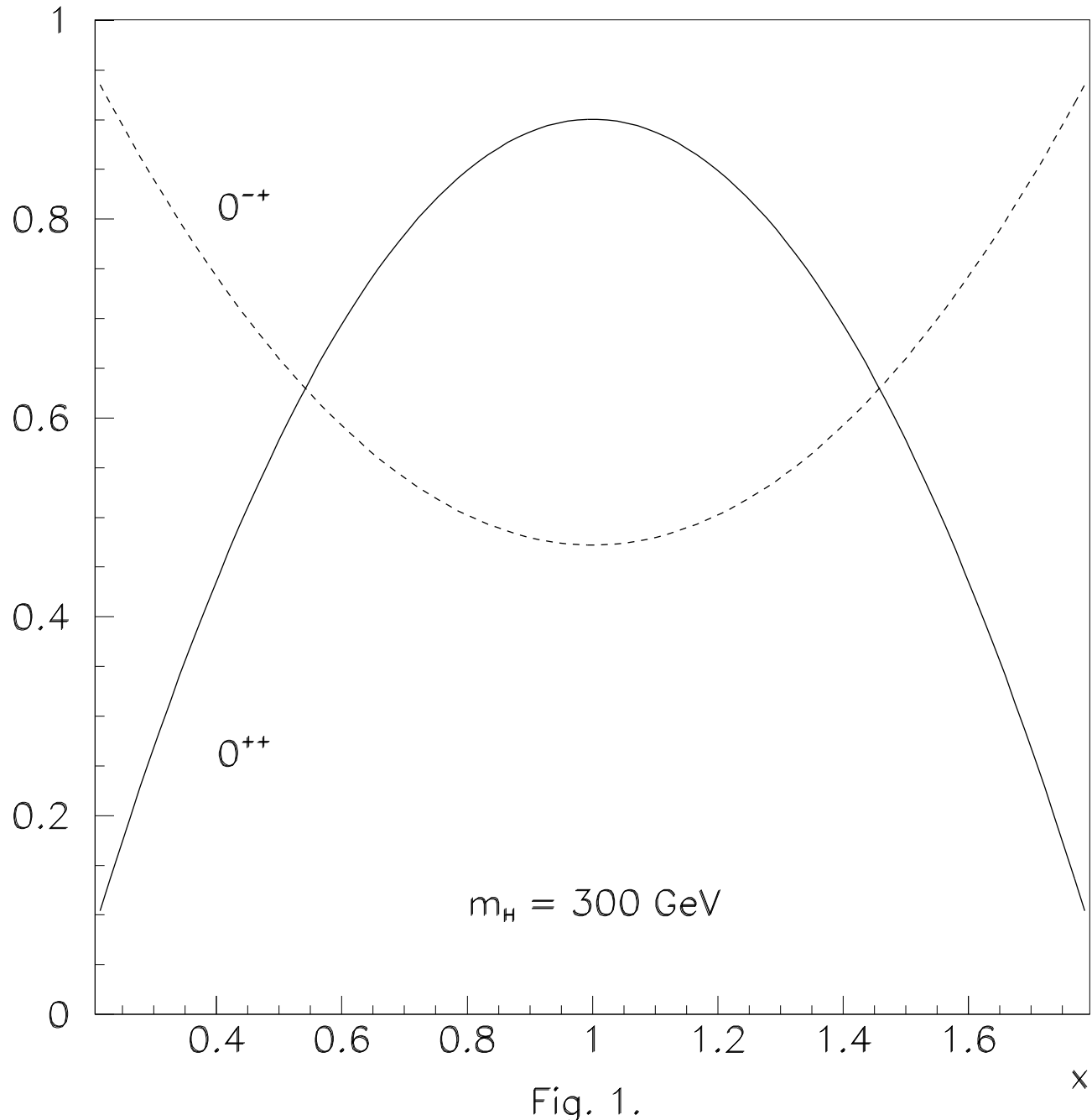


Fig. 1.

$H \rightarrow ZZ \rightarrow \mu^+\mu^-\mu^+\mu^-$   
(scalar)

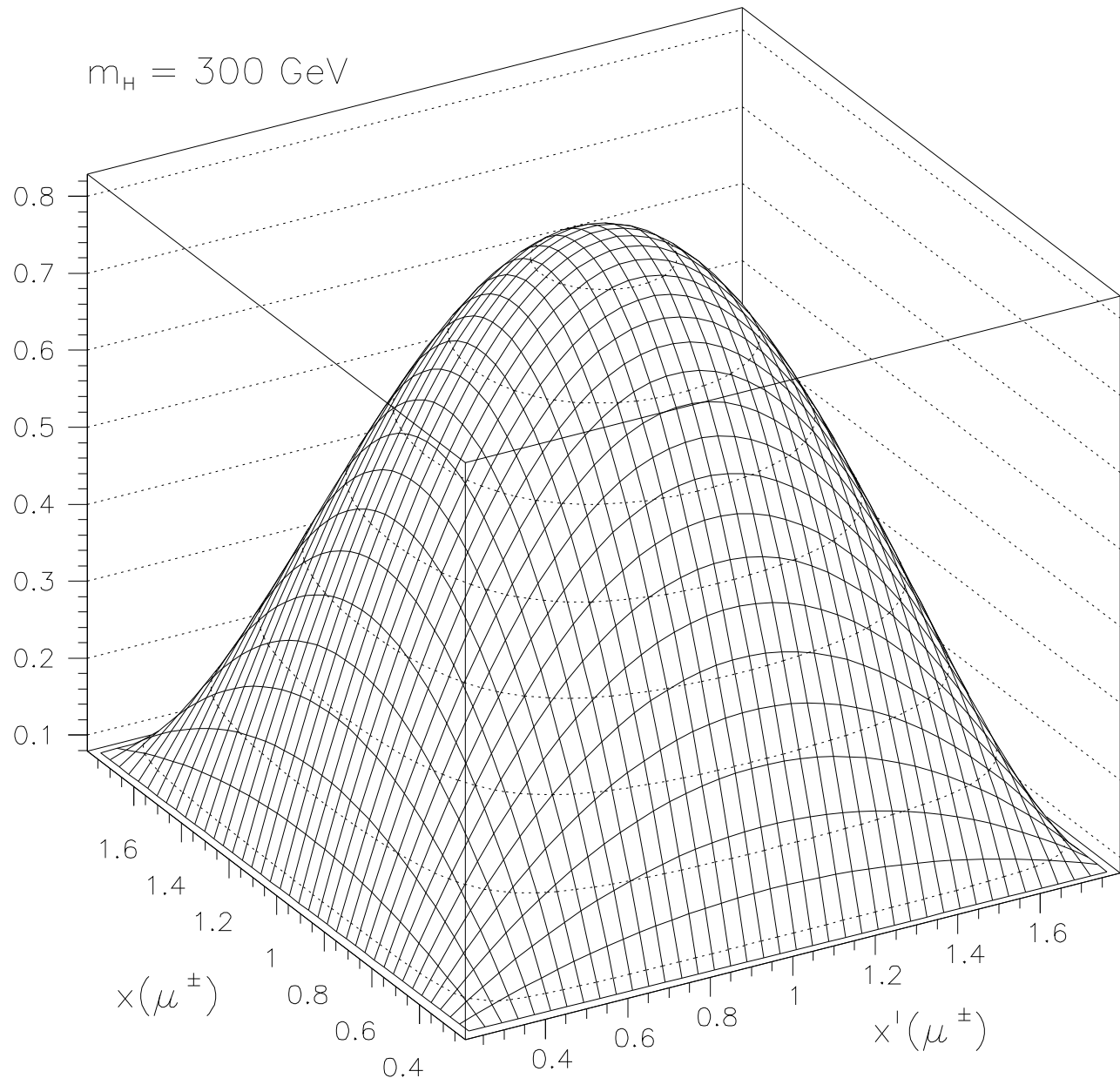


Fig. 2(a).

$H \rightarrow ZZ \rightarrow \mu^+\mu^-\mu^+\mu^-$   
 (pseudoscalar)

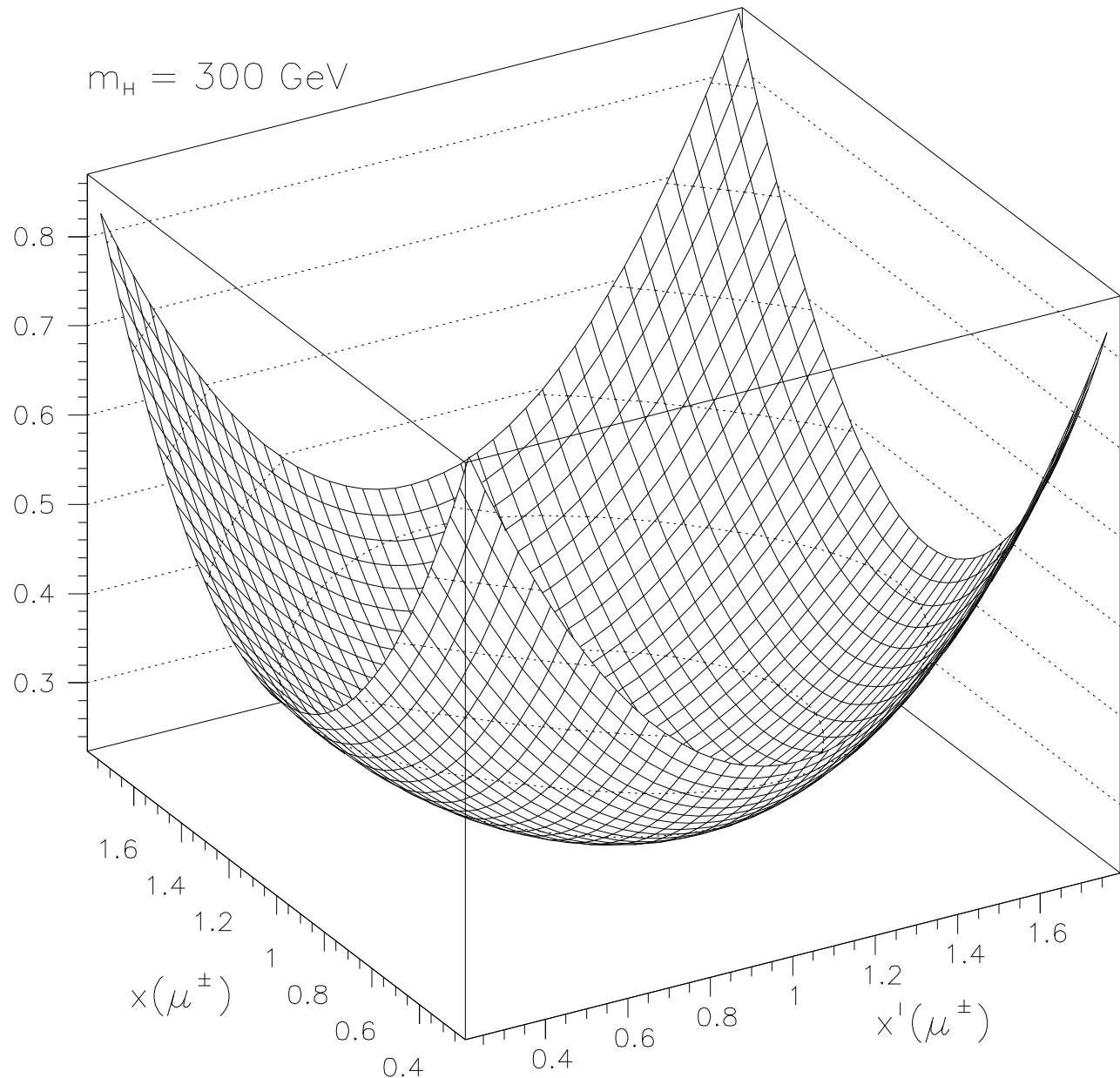


Fig. 2(b).

$H \rightarrow ZZ \rightarrow \mu^+\mu^-\mu^+\mu^-$   
 (scalar)

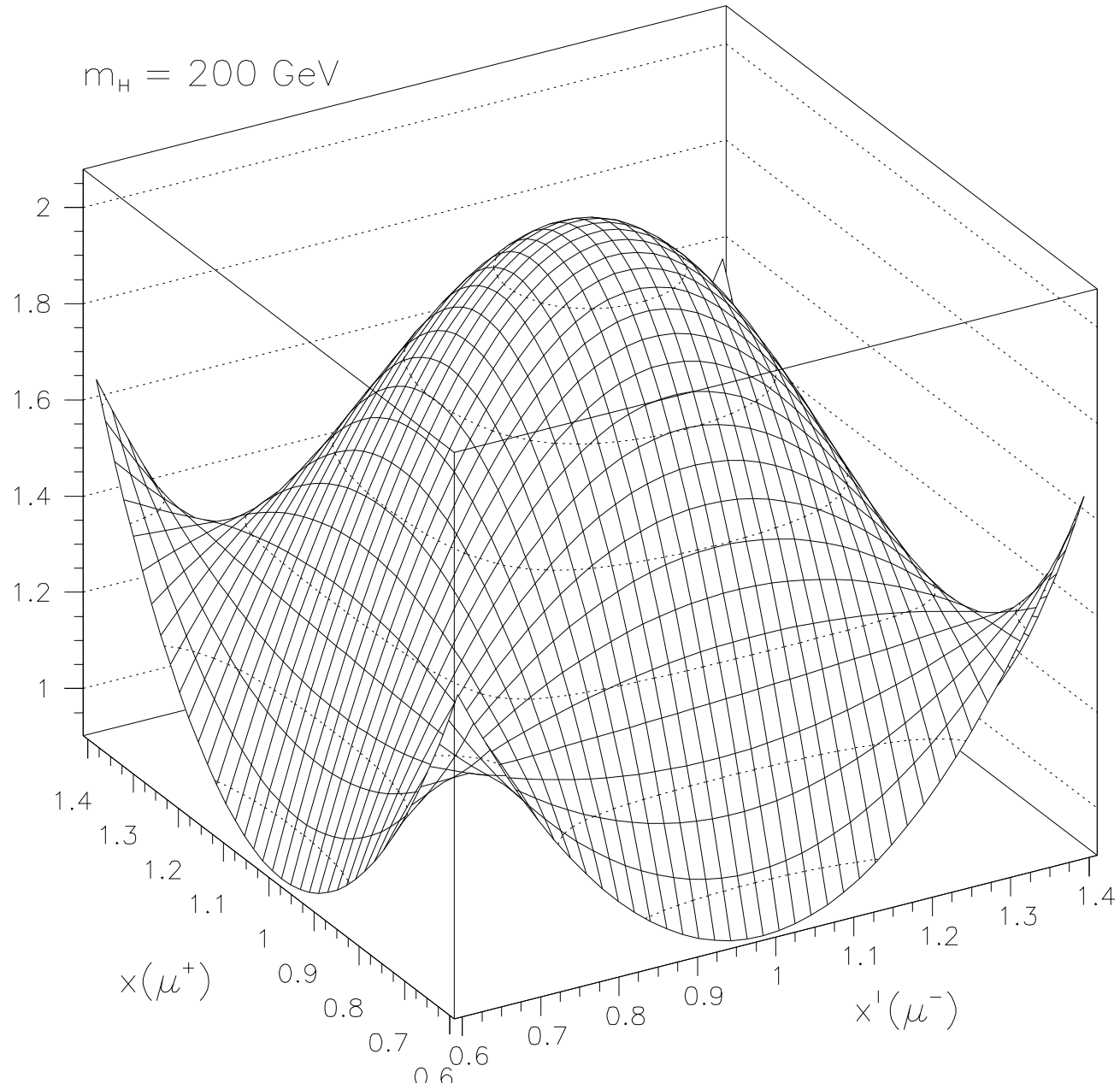


Fig. 3(a).

$$\begin{aligned}
 H \rightarrow W^+W^- \rightarrow \mu^+\nu_\mu\mu^-\bar{\nu}_\mu \\
 (\text{scalar})
 \end{aligned}$$

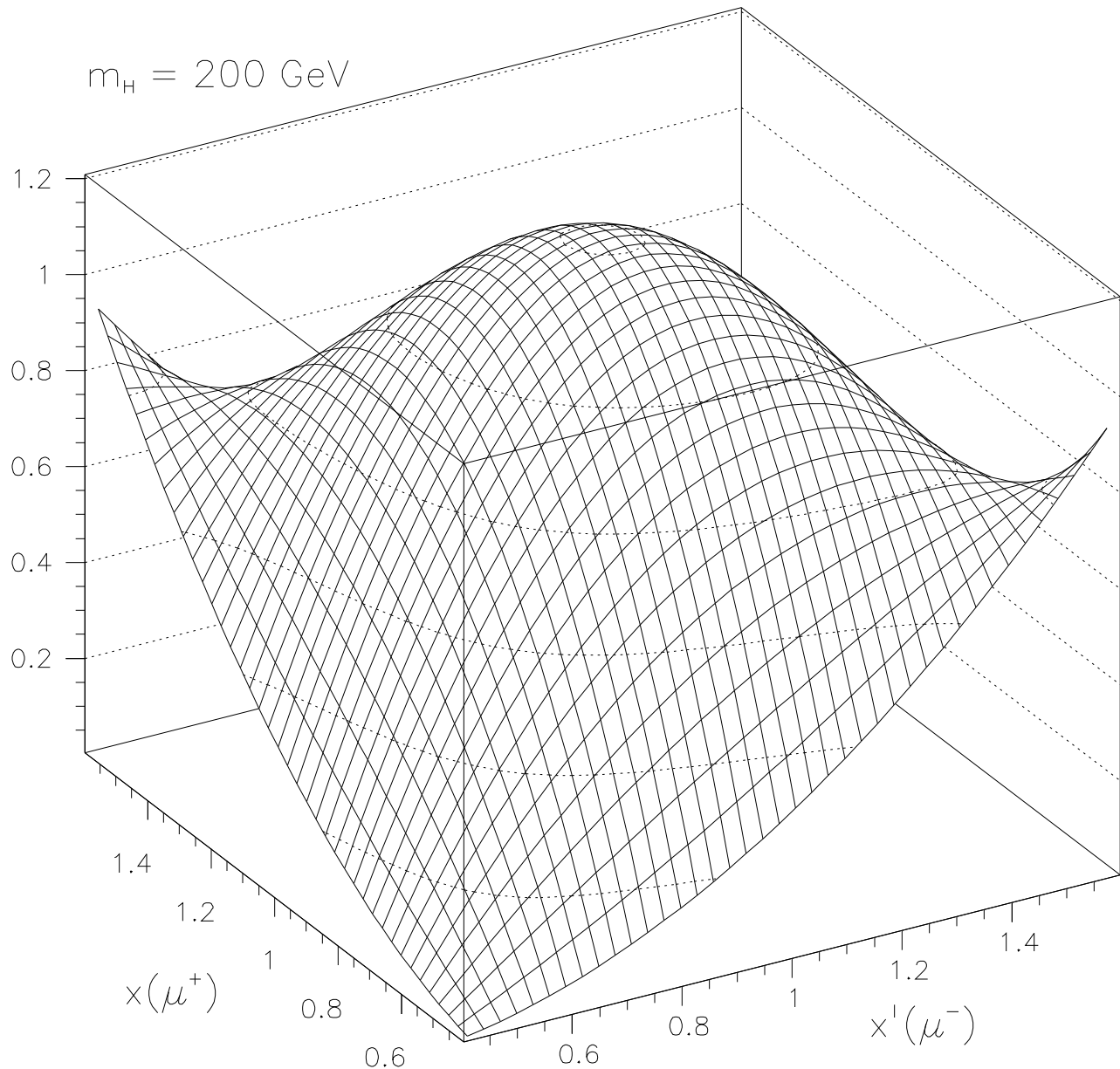


Fig. 3(b).

$$H \rightarrow ZZ \rightarrow \mu^+ \mu^- \mu^+ \mu^-$$

(pseudoscalar)

$m_H = 200$  GeV

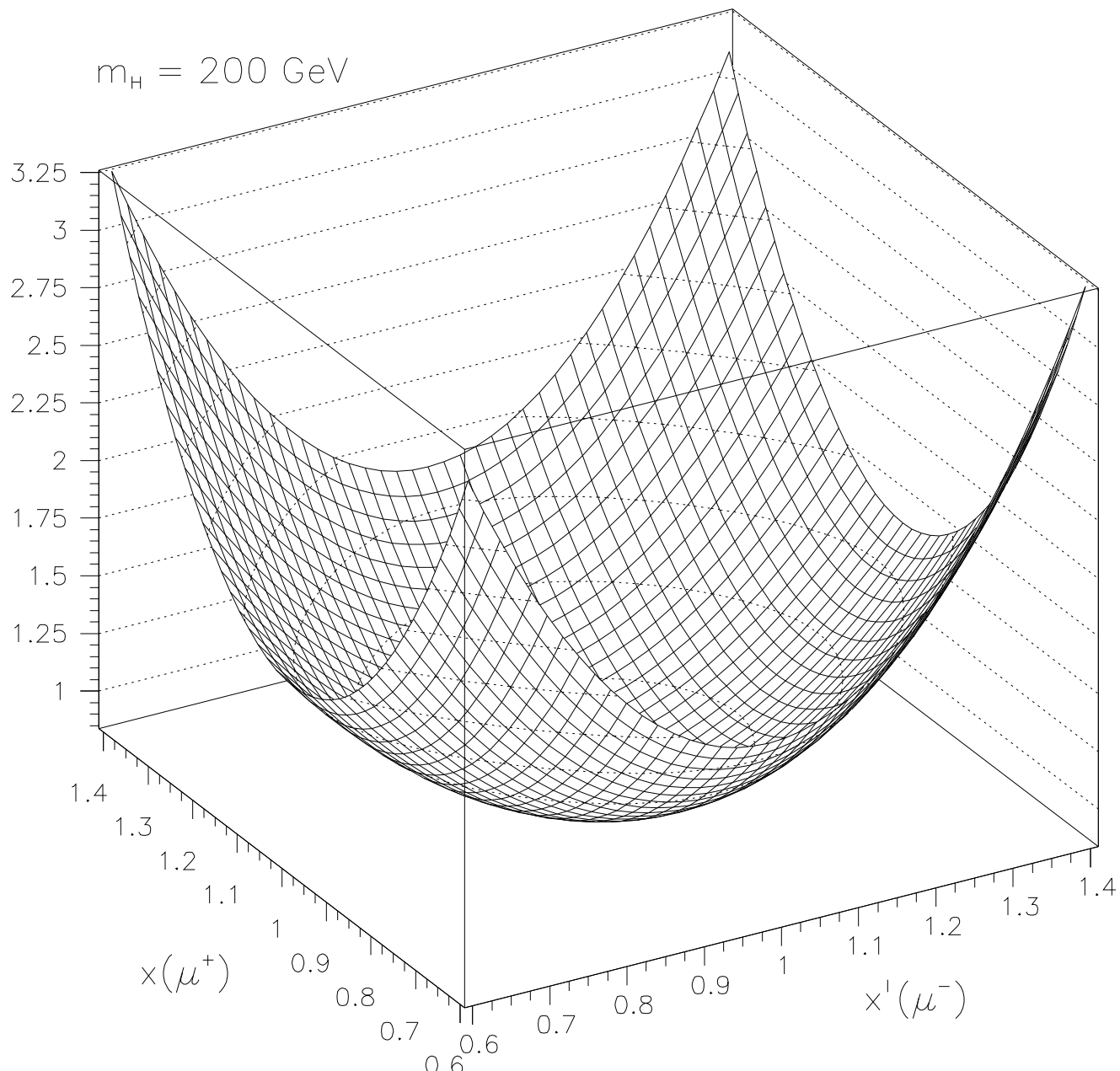


Fig. 4(a).

$H \rightarrow W^+W^- \rightarrow \mu^+\nu_\mu\mu^-\bar{\nu}_\mu$   
 (pseudoscalar)

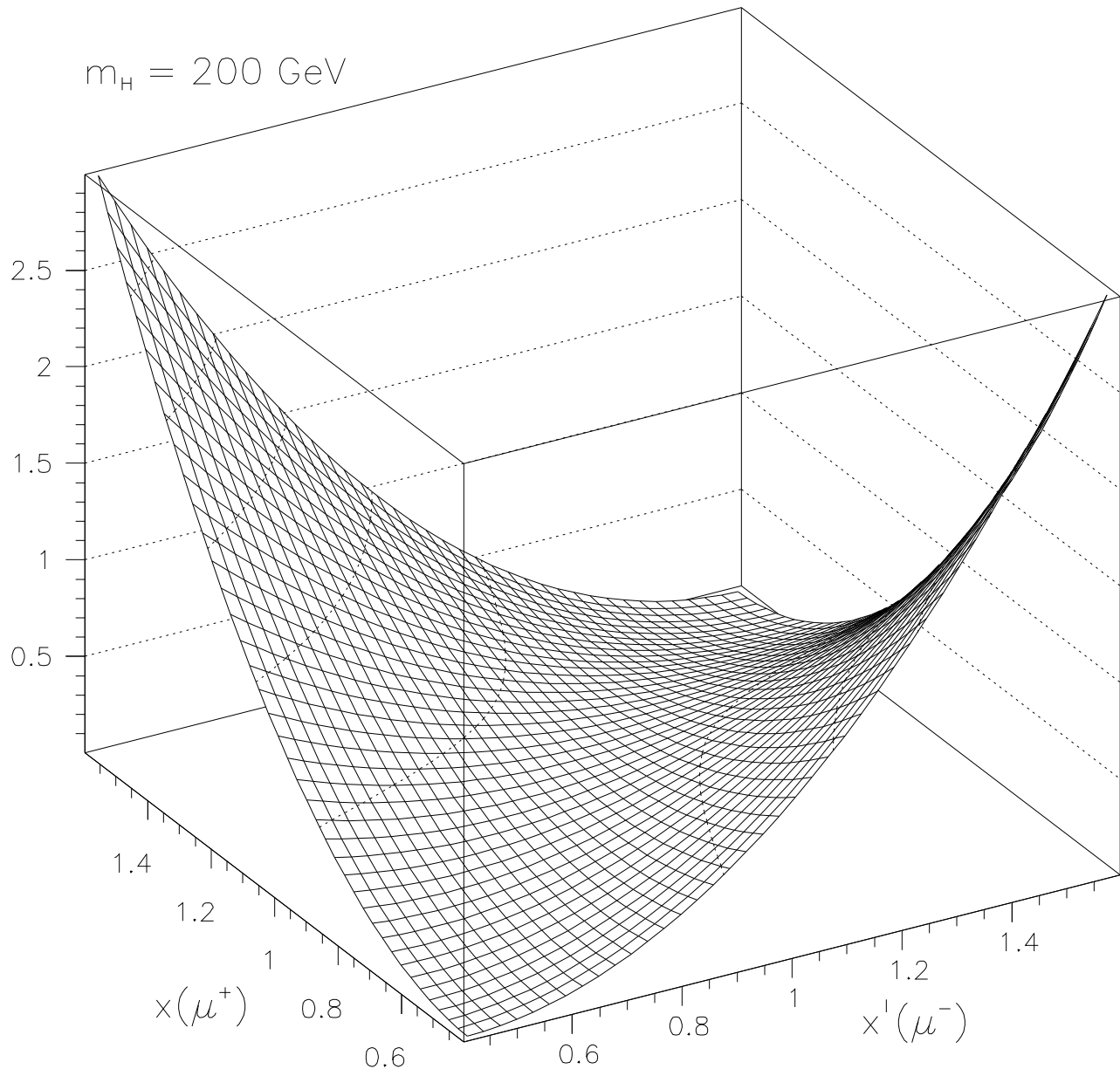


Fig. 4(b).